

STUDY OF THE LONGITUDINAL INSTABILITY OF RELATIVISTIC ELECTRON RINGS

B. S. GETMANOV and V. G. MAKHANKOV

Joint Institute for Nuclear Research, Moscow, USSR

(Received January 13, 1976; in final form October 19, 1976)

The theory is presented of the longitudinal instability of relativistic electron rings (RER) in the thin ring model, allowing for any (not only small) deviation of the rotational frequency of the perturbing particles from the average initial frequency, and taking into account both imaginary and real parts of the impedance. The influence of nonlinear effects on the development of the longitudinal instability of the RER is studied both analytically and numerically. It is shown that in free space this phenomenon may retard the instability development, but not sufficiently for its stabilization. For a beam enclosed in a chamber nonlinear stabilization appears possible. Comparison with experimental results is presented for this case.

1 INTRODUCTION

Different kinds of instabilities of the relativistic electron rings (RER)^{1,2} are the main obstacles on the way to the effective realization of the idea of using these rings for collective acceleration of ions. The longitudinal (azimuthal) instability (LI) seems to be the most dangerous one. It has a hydrodynamic nature and manifests itself in the grouping of the ring particles in clusters ("bunches") ["negative mass" instability (NMI)].³ This instability also manifests itself in induced coherent synchrotron radiation ("radiational instability").⁴ This instability has a threshold⁵ corresponding to the range of energies ΔE , the rms energy spread (and the range of radius which results from the relativistic relation between energy E and rotational frequency ω : $\omega = ecB/E$, (where B is the magnetic field). The efficiency of acceleration in the regime below the threshold of the instability ($\Delta E > \Delta E_{cr}$) does not exceed the efficiency which has been achieved with ordinary accelerators⁶ (at least for light ions). On the other hand, equations which describe the dynamics of the instability of RER's are nonlinear, and one may expect that nonlinear interactions can limit the level of the perturbing fields, slow down the process and even prevent the instability, or that they can lead to its nonlinear stabilization.^{7,8} The longitudinal instability has been observed experimentally both in the creation of the E -layer⁹ and in experiments with RER's.^{10,11} Damping of the coherent radiation after the characteristic splash at the initial

stage of instability development supports the supposition of the importance of nonlinear effects which limit the amplitudes of the perturbing fields and the fluctuations of the beam density.

It is important to choose a good model for theoretical analysis of the longitudinal instability in RER's. Most commonly used is the thin ring model,³ in which the interaction between longitudinal and transverse perturbations is neglected, and the problem reduces to a one-dimensional one. Even in this simple model, analytical study of the longitudinal instability with nonlinear interactions meets with considerable difficulties, in particular because of the absence of a small parameter in the problem.¹² A simplified "quasi-kinetic" description of the instability is given in Ref. 13 within the frame of this model. The authors predict an asymptotic behavior of the ring at the instability saturation stage and, according to their predictions, the parameters of the ring, ΔE in particular, are in any case not better at this stage than for the stable ring, i.e., $\Delta E > \Delta E_{cr}$. However, in these papers the real part of the impedance which is responsible for the radiation of the ring was neglected, as well as an important physical effect of energy mixing for different harmonics. The latter effect can lead to considerable retardation of the instability development process, if not to stabilization.^{7,8} From our point of view, only numerical methods provide the possibility of complete analysis of the dynamics of the instability. The radiational instability dynamics of the ring in free space were studied numerically in Ref. 11.

However, no clear answer was obtained to the question of what is the role of nonlinear interactions and whether or not nonlinear stabilization of the longitudinal instability is possible.

In this paper we study the longitudinal instability in RER's using the thin ring model and numerical and analytical methods. Much attention is given to analysis of the influence of nonlinear interactions. Some new results of the longitudinal instability theory are presented in Section 2, the qualitative character of the longitudinal instability development is discussed in Section 3, formulation of the numerical simulation problems will be found in Section 4, and Sections 5 and 6 contain the results of this numerical simulation for the ring in free space and in an enclosing chamber.

2 ANALYTICAL THEORY

One usually assumes that the deviations of the particles' rotational frequency from the average initial frequency $\omega_0 = eB/mc\gamma_0$ are small in order to obtain Vlasov's equation for the one-dimensional energy distribution function in the "negative mass" instability theory.³ This assumption is not bad for the study of the negative mass instability in regimes which are not too much above the critical one. However, it turns out to be unsatisfactory in the theory of the longitudinal instability which takes radiation into account.

In the thin ring theory we start from the equation

$$\frac{\partial \psi}{\partial t} + \dot{\phi} \frac{\partial \psi}{\partial \phi} + \dot{W} \frac{\partial \psi}{\partial W} = 0 \quad (2.1)$$

for the electron distribution function in (ϕ, W) phase space of the azimuth angle and corresponding generalized momentum. In (2.1)

$$\dot{\phi} = \omega(W) = \frac{eB}{mc\gamma(W)} = \frac{eBc}{E(W)} \quad (2.2)$$

is the rotational frequency of the particle with canonical momentum W in the constant uniform magnetic field B , $E = mc^2\gamma$.

W can be determined from Hamilton's equation

$$\dot{\phi} = \frac{\partial H}{\partial W}. \quad (2.3)$$

H is the particle energy, expressed as a function of momentum, so we have from (2.2) and (2.3):

$$W(E) = \int_{E_0}^E \frac{dE}{\dot{\phi}} = \frac{1}{2} \frac{E^2 - E_0^2}{ecB}. \quad (2.4)$$

Here by field B we mean the sum of external magnetic field B_{ext} and the beam's own average magnetic field B_b , which we can assume to be uniform along ϕ and constant in time.

The constant E_0 we shall put equal to the energy of the particle with the average initial rotational frequency ω_0 . Henceforth we shall attach index "0" to the quantities corresponding to the particle on the orbit with frequency $\omega_0(E_0, R_0, \gamma_0)$. In particular, $W_0 = 0$. Therefore, we have

$$W = \frac{1}{2} \frac{(mc^2)^2(\gamma^2 - \gamma_0^2)}{ecB} = \frac{1}{2} \frac{mcR_0(\gamma^2 - \gamma_0^2)}{\gamma_0\beta_0}. \quad (2.5)$$

($\beta = v/c$, R is the orbit's radius). When

$$\frac{\Delta\gamma}{\gamma_0} = \frac{|\gamma - \gamma_0|}{\gamma_0} \ll 1, \quad \beta \simeq 1,$$

we have

$$W = mcR_0\Delta\gamma,$$

which differs from the definition used in Refs. 13 and 14 by a factor of 2π .

By definition, the effective mass of the particle is

$$\begin{aligned} M &= \frac{dW}{d\dot{\phi}} = \frac{dW}{dE} \frac{dE}{d\omega} = -\frac{1}{\dot{\phi}} \frac{E}{\omega} \\ &= -\frac{E}{\omega^2} = -\frac{m\gamma R^2}{\beta^2}. \end{aligned} \quad (2.6)$$

Introducing the reciprocal mass $\alpha_0 = M_0^{-1}$ and using (2.4) we derive the following expression for the energy of the particle in a ring:

$$E = \sqrt{E_0^2 + 2E_0\omega_0 W} = -\frac{\omega_0^2}{\alpha_0} \sqrt{1 - \frac{2\alpha_0 W}{\omega_0}}, \quad (2.7)$$

and for its Hamiltonian:

$$\begin{aligned} H = T + V(\phi) &= -\frac{\omega_0^2}{\alpha_0} \sqrt{1 - \frac{2\alpha_0 W}{\omega_0}} \\ &+ 2\pi R_0 e \int \mathcal{E}(\phi, t) d\phi, \end{aligned} \quad (2.8)$$

where $\mathcal{E}(\phi, t)$ is the azimuthal perturbing electric field, averaged over the cross section of the ring.

Using (2.5) it is easy to show that W , as defined by the formula (2.4), coincides with the usual generalized momentum

$$W = RP_\phi - \frac{e}{c} RA_\phi^{(0)} = M - \frac{e}{c} RA_\phi^{(0)} \quad (2.9)$$

of the particle in the constant uniform magnetic field B . Here $P_\phi = mc\beta\gamma$ is the azimuthal momentum, \mathbf{A} has only the component $A_\phi = \frac{1}{2}BR$ and $E_0 = mc^2$, i.e., $\gamma_0 = 1$. The transition to $W(E, E_0)$ with $\gamma_0 \neq 1$ corresponds to the gradient transformation of the vector potential.

The ‘‘kinetic’’ part of the Hamiltonian (2.8) coincides with the kinetic part of the traditional Hamiltonian of the charged particle in the magnetic field

$$H = c \sqrt{m^2 c^2 + \frac{1}{R^2} \left(W + \frac{e}{c} R A_\phi \right)^2}$$

in the ‘‘adiabatic’’ approximation $(dR/dt)(1/\omega_0 R) \ll 1$. Formula (2.2) for the nonequilibrium particle in a ring is valid in the same approximation.

From Eq. (2.8) it is easy to show that

$$\frac{\partial H}{\partial W} = \dot{\phi} = \frac{\omega_0}{\sqrt{1 - \frac{2\alpha_0 W}{\omega_0}}}, \quad (2.10)$$

$$-\frac{\partial H}{\partial \phi} = \dot{W} = 2\pi \operatorname{Re} \mathcal{E}. \quad (2.11)$$

Expanding (2.8) and (2.10) in powers of $\alpha_0 W/\omega_0$, we have

$$\begin{aligned} T &\simeq -\frac{\omega_0^2}{\alpha_0} + \omega_0 W + \frac{\alpha_0 W^2}{2} \\ &= -\frac{3}{2} \frac{\omega_0^2}{\alpha_0} + \frac{1}{2\alpha_0} (\omega_0 + \alpha_0 W)^2 \xrightarrow{W \rightarrow 0} mc^2 \gamma_0 \end{aligned} \quad (2.12)$$

$$\dot{\phi} \simeq \omega_0 + \alpha_0 W + \dots \quad (2.13)$$

The second term in (2.12) coincides with the kinetic part of the Hamiltonian from Ref. 13 and leads to the right equation of motion (2.13) in the approximation

$$\left| \frac{\alpha_0 W}{\omega_0} \right| \ll 1.$$

But it gives the wrong expression for the total energy of the particle in the ring. Nevertheless, in the negative mass instability theory this term allows us to obtain the conservation of energy,¹³ because it gives the right description of the ‘‘heat’’ motion of the particles.

The Fourier transform of (2.1) is

$$\frac{\partial \psi_n}{\partial t} + in\dot{\phi}\psi_n + 2\pi e R_0 \sum_{m=-\infty}^{\infty} \mathcal{E}_m(t) \frac{\partial \psi_{n-m}}{\partial W} = 0. \quad (2.14)$$

Introducing the coupling impedance Z_m by the formula

$$e\mathcal{E}_m = Z_m \frac{e^2 c}{(2\pi R_0)^2} \lambda_m, \quad (2.15)$$

where $\lambda_m = \int \psi_m dW$, we obtain

$$\begin{aligned} \partial_t \psi_n + \frac{in\omega_0}{\sqrt{1 - \frac{2\alpha_0 W}{\omega_0}}} \psi_n \\ + \frac{e^2 c}{2\pi R_0} \sum_m Z_m \lambda_m \partial_W \psi_{n-m} = 0. \end{aligned} \quad (2.16)$$

If $|\alpha_0 W/\omega_0| \ll 1$ it follows from (2.16) that

$$\begin{aligned} \partial_t \psi_n + in(\omega_0 + \alpha_0 W) \psi_n \\ + \frac{e^2 c}{2\pi R_0} \sum_m Z_m \lambda_m \partial_W \psi_{n-m} = 0. \dagger \end{aligned} \quad (2.17)$$

We now normalize the distribution function to the total number of electrons in the ring

$$\int \psi dW d\phi = N. \quad (2.18)$$

Then for zero harmonic we have

$$\int \psi_0(W, t) dW = \frac{N}{2\pi}. \quad (2.19)$$

To analyze the ring’s energy balance, we average the quantity $T + \frac{1}{2}V$ over the variables W and ϕ with weight $\psi(\phi, W, t)$. The factor $\frac{1}{2}$ in front of V appears as a result of the two-particle nature of the interaction:¹³ ‡

$$E(t) = E_p(t) + E_i(t)$$

$$\begin{aligned} &= \frac{2\pi\omega_0^2}{|\alpha_0|} \int_{W_{\min}}^{\infty} \psi_0(W) \sqrt{1 + \frac{2|\alpha_0|W}{\omega_0}} dW \\ &\quad - \frac{e^2 c}{2R_0} \sum_n \frac{Z_n''}{n} |\lambda_n|^2. \end{aligned} \quad (2.20)$$

Here and later in the paper we shall denote the real part of a complex number by one prime,

† We shall often consider Eq. (2.17) with $\omega_0 = 0$, i.e., for the function $\tilde{\psi}_n = \psi_n e^{in\omega_0 t}$ (distribution centered at ω_0).

‡ A similar expression, although not exactly correct, was obtained in Ref. 14. It was erroneously stated that the quantity $E(t)$ is constant in time. Actually, $E(t)$ is conserved only if $Z_n'' = 0$ (see below).

and the complex part by two primes; $W_{\min} = -mcR_0\beta_0\gamma_0$. Note that by virtue of the Fourier-transform properties $Z_{-n} = Z_n^*$, or $Z'_{-n} = Z'_n$, $Z''_{-n} = -Z''_n$. Expression (2.20) does not contain the term

$$i \sum \frac{Z'_n}{n} |\lambda_n|^2,$$

which is equal to zero.

At the initial moment of time, if $\lambda_n \rightarrow 0$, the ring's energy is

$$E_0(0) \simeq N \frac{\omega_0^2}{|\alpha_0|} - \frac{1}{2} N |\alpha_0| \langle W_0^2 \rangle, \quad (2.21)$$

where

$$\begin{aligned} \langle W_0^2 \rangle &= \int W^2 \psi \, dW \, d\varphi / \int \psi \, dW \, d\varphi \\ &= \frac{2\pi}{N} \int \psi_0 W^2 \, dW, \end{aligned} \quad (2.22)$$

and $\langle W \rangle = \langle W_0^2 \rangle^{1/2}$ is the initial semi-dispersion of the beam (we assume that $\psi_0(W)$ is symmetric with respect to W , so that $\int W \psi_0 \, dW = 0|_{t=0}$).

In the limit of an infinitely thin ring $\langle W_0 \rangle \rightarrow 0$, its energy $E(0) \rightarrow Nmc^2\gamma_0$ according to (2.12).

To find the power of the ring radiation, we calculate the quantity

$$\begin{aligned} \frac{dE}{dt} &= \frac{2\pi\omega_0^2}{|\alpha_0|} \int \sqrt{1 + \frac{2|\alpha_0|W}{\omega_0}} \partial_t \psi_0 \, dW \\ &\quad - \frac{e^2c}{2R_0} \sum_n \frac{Z''_n}{n} \left(\lambda_n \frac{d\lambda_{-n}}{dt} + \lambda_{-n} \frac{d\lambda_n}{dt} \right). \end{aligned}$$

Using Eq. (2.16) we obtain

$$\partial_t \psi_0 = -\frac{e^2c}{2\pi R_0} \sum_n Z_n \lambda_n \frac{\partial \psi_{-n}}{\partial W}$$

and

$$\frac{d}{dt} \lambda_n = -in\omega_0 \int \left(1 + \frac{2|\alpha_0|W}{\omega_0} \right)^{-1/2} \psi_n \, dW.$$

Substituting these relations in the expression for dE/dt and integrating by parts we conclude, finally:

$$\begin{aligned} \frac{dE}{dt} &= \frac{e^2c\omega_0}{2R_0} \\ &\quad \times \left\{ \sum_n iZ''_n \left[\lambda_n \int \left(1 + \frac{2|\alpha_0|W}{\omega_0} \right)^{-1/2} \psi_{-n} \, dW \right. \right. \\ &\quad \left. \left. + \lambda_{-n} \int \left(1 + \frac{2|\alpha_0|W}{\omega_0} \right)^{-1/2} \psi_n \, dW \right] \right. \\ &\quad \left. + 2 \sum_n Z'_n \lambda_n \int \left(1 + \frac{2|\alpha_0|W}{\omega_0} \right)^{-1/2} \psi_{-n} \, dW \right\}. \end{aligned} \quad (2.23)$$

In the case of the negative mass instability, $Z'_n = 0$, $Z''_n < 0$ and, substituting $n \rightarrow -n$ in the second term of (2.23), we will derive the energy conservation law¹³ $dE/dt = 0$.

When $Z'_n \neq 0$ we have

$$\frac{dE}{dt} = \frac{e^2c\omega_0}{R_0} \sum_n Z'_n \lambda_n \int \left(1 + \frac{2|\alpha_0|W}{\omega_0} \right)^{-1/2} \psi_{-n} \, dW. \quad (2.24)$$

Since both in free space and in enclosing chambers $Z'_n < 0$, Eq. (2.24) describes the energy losses of the ring due to radiation. When

$$\left| \frac{\alpha_0 W}{\omega} \right| \ll 1,$$

we have two independent equations for the moments of the distribution function, instead of the one formula (2.24):

$$\frac{d}{dt} \int W \psi_0 \, dW = \frac{e^2c}{2\pi R_0} \sum_n Z'_n |\lambda_n|^2 \quad (2.25)$$

[see (2.17)], and

$$\begin{aligned} \frac{d}{dt} \left[\int \frac{|\alpha_0|W^2}{2} \psi_0 \, dW + \frac{e^2c}{4\pi R_0} \sum_n \left(\frac{Z''_n}{n} \right) |\lambda_n|^2 \right. \\ \left. = \frac{e^2c}{2\pi R_0} |\alpha_0| \sum_n Z'_n \lambda_n \int W \psi_{-n} \, dW \right]. \end{aligned} \quad (2.26)$$

The first of these relations determines a change in the ring's average momentum due to radiation, the second indicates the change of the sum of "kinetic" (thermal) and potential energies of the ring. Equation (2.25) has an obvious physical meaning: radiation power is proportional to the product of the square of the "current" $|\lambda_n|^2$ and resistance Z'_n . The quantity $\int W \psi_0 \, dW$ is pro-

portional to the decrease of the average ring's radius (since $Z'_n < 0$), therefore a symmetrical ($\int W\psi_0 dW = 0$) initial distribution in the case of a negative mass instability ($Z'_n = 0$) will later remain the same.

In what follows we will be interested in the behaviour of the ring in the resonator where the relation between Z'_n and Z''_n (in particular, its sign) may change with radius. It seems to be appropriate to present here exact formulas for the increments and thresholds of a longitudinal instability. In the hydrodynamic limit¹⁵

$$\gamma_n = n\omega_0 \sqrt{\frac{2v}{\gamma_0}} \sqrt{\frac{|Z'_n| - Z''_n}{2nZ_0}}, \quad (2.27)$$

where $v = (e^2/mc^2)(N/2\pi R_0)$ is the Budker parameter: $(v/\gamma_0) \ll 1$, and

$$\left(\frac{\Delta E}{E}\right)_{\text{cr}} = \sqrt{\frac{2v}{\gamma_0}} \sqrt{\frac{|Z'_n| - Z''_n}{2nZ_0}}. \quad (2.28)$$

In conclusion, we present the estimate for the amplitude of the induced fields at the saturation stage from Ref. 12:

$$\mathcal{E}_n \lesssim \frac{mc^2 v}{eR_0} n^{1/3} \left(\left| \frac{Z'_n}{nZ_0} \right| = n^{-2/3} \right). \quad (2.29)$$

We shall use it for comparison.

3 QUALITATIVE ANALYSIS OF THE SOLUTIONS OF THE SYSTEM (2.14)

It is appropriate to trace first some qualitative features of the solutions of the system (2.14) to simplify interpretation of the results of numerical calculations, and for their better understanding.

a) Let us consider the truncated system (2.17) for $n = 0, 1$ (it is easy to generalize all the arguments for the case of arbitrary n). We rewrite it in the real form:

$$\begin{aligned} \partial_t \psi_0 &= -2(A_1 \partial_W \psi'_1 + B_1 \partial_W \psi''_1) \\ \partial_t \psi'_1 &= \alpha_0 W \psi'_1 - A_1 \partial_W \psi_0 \\ \partial_t \psi''_1 &= -\alpha_0 W \psi''_1 - B_1 \partial_W \psi_0. \end{aligned} \quad (3.1)$$

Here

$$A_1 = \sigma'_1 \lambda'_1 - \sigma''_1 \lambda''_1; \quad B_1 = \sigma'_1 \lambda''_1 + \sigma''_1 \lambda'_1;$$

$$\sigma_n = \frac{e^2 c}{2\pi R_0} Z_n.$$

We differentiate the first equation of (3.1) again and substitute in it expressions for $\partial_t \psi'_1, \partial_t \psi''_1$ from the second and third equations:

$$\begin{aligned} \partial_t^2 \psi_0(W) &= C^2 \partial_W^2 \psi_0 - 2(\partial_t A_1 \partial_W \psi'_1 + \partial_t B_1 \partial_W \psi''_1) \\ &\quad - 2\alpha_0 [A_1 \partial_W (W \psi''_1) - B_1 \partial_W (W \psi'_1)]. \end{aligned} \quad (3.2)$$

Here

$$\begin{aligned} C^2 &= 2(A_1^2 + B_1^2) = 2(\sigma_1'^2 + \sigma_1''^2)(\lambda_1'^2 + \lambda_1''^2) \\ &= 2|\sigma_1|^2 |\lambda_1|^2. \end{aligned}$$

In the general case where $n > 1$

$$C^2 = \sum_n 2|\sigma_n|^2 |\lambda_n|^2.$$

We need Eq. (3.2) to understand qualitatively the behaviour of the function $\psi_0(W, t)$ at the initial stage of instability development, when the fields are small and we can neglect nonlinear terms in the system (2.17) (if $n = 1$ they fall out automatically).

The second term on the right-hand side of (3.2) can be presented in a form analogous to that of the first term if $\psi_{n \neq 0}(W)$ is expressed through the $\psi_0(W)$ from (2.17), assuming that the dispersion relation of the linear theory is valid and neglecting nonlinear terms:

$$\psi_n = -i \frac{\lambda_n \sigma_n \partial_W \psi_0}{\omega_n - n\alpha_0 W}. \quad (3.3)$$

This relation is valid for $t = 0$, and it is valid with good accuracy in the linear stage of the instability development. When $\omega_n \gg |nW\alpha_0|$, $\psi_n \sim \partial_W \psi_0$, then the second term on the right-hand side of (3.2) can be written as $C_1 \partial_W^2 \psi_0$. It can be shown that the third term on the right-hand side of (3.2) is smaller than the first two, and we will neglect it. Then (3.2) takes the form:

$$\partial_t^2 \psi_0(W) = C_0^2 \partial_W^2 \psi_0(W), \quad (3.4)$$

where $C_0^2 = C^2 + C_1$.

The formal solution of (3.4) is [if $t \cdot dC_0/dt \ll C_0(t)$]:

$$\begin{aligned} \psi_0(W, t) &= \frac{\varphi(W + C_0 t) + \varphi(W - C_0 t)}{2} \\ &\quad + \frac{t}{2C_0} \int_{W-C_0 t}^{W+C_0 t} \eta(\zeta) d\zeta. \end{aligned} \quad (3.5)$$

Here

$$\varphi(W) = \psi_0(W)|_{t=0}; \quad \eta(W) = \partial_t \psi_0|_{t=0}.$$

The second term of (3.5) is always small in comparison with the first one ($C_0^2 = 2 \sum |\lambda_n|^2 |\sigma^n|^2$ grows fast with the instability development). It follows from (3.5) that the initial distribution $\psi_0(W)$ symmetrically "crawls away" with increasing speed into two similar distributions, i.e., the ring splits into two rings.

The above considerations are, of course, *very crude and qualitative in nature*; they might be justified by the fact that the described phenomena were observed in a more or less well-expressed form in practically all of the numerical experiments (see below). This effect is best seen when the initial dispersion is small (in the strongly above-critical regimes, corresponding to the approximation $\omega_n \gg n\alpha_0 W$), and it is maximum in the case $Z'_n = 0$, when there is no radiation. Then the distribution function rapidly becomes "two-humped," remaining symmetrical with respect to the center of the distribution. Such a behaviour of $\psi_0(W)$ is preserved for a considerable time even in the nonlinear stage of the instability development, which is rather surprising.

Actually, of course, the ring as a whole does not split into two rings. As a result of the negative mass instability it breaks into separate bunches, which have small electron concentration at the average radius. When we take the average along the azimuth, we find the picture described above.

b) Equation (2.1) is Vlasov's kinetic equation without collisions; numerical study of it leads to the specific difficulties,⁸ which we will now consider. Let us formally integrate (2.17) in the linear approximation:

$$\begin{aligned} \psi_n(x, t) = & \partial_x \psi_0 \sigma_n \int_0^t \exp[in\alpha_0 x(t-t')] \lambda_n(t') dt' \\ & + \varphi_n \exp[-in\alpha_0 xt]. \end{aligned} \quad (3.6)$$

Here x is the dimensionless generalized moment, which is introduced for the purpose of numerical study, $\phi_n(x) = \psi_n(x)|_{t=0}$. From Eq. (3.6) it follows that the solution has an oscillating part with a wavelength decreasing in time, [$\lambda = (n\alpha_0 t)^{-1}$]. Therefore, the computer time is limited in principle, because λ cannot be smaller than the step in x . Nonlinear effects lead to an increase of oscillation amplitude and to appearance of the captured particles, which, in turn, leads to oscillations of the oscillations of the distribution function ψ_0 . This phenomenon was observed in Ref. 14 and in all of our numerical experiments. In the cases when

the time is large, it leads to important distortion of the distribution function. The oscillations appear only on the microscopic level and they are connected with the tendency of the distribution function to produce in the course of time sharp gradients in the phase space when there is no viscosity. They should not contribute to the macroscopic, measurable quantities, which are given by the moments of the distribution function. Note that the term of the type may describe the real phenomenon of "plasma echo," which has been observed experimentally.¹⁶

Different dissipative terms were introduced into the right-hand side of Eq. (2.17) and tested in order to suppress oscillations on the boundaries of the domain of variation of the distribution function. We chose the damping in the form $\bar{v}\psi_n(x, t) = -\mathcal{E}f(n, x)\psi_n(x, t)$, where \mathcal{E} changes from 10^{-4} to 10^{-1} , and $f(n, x)$ is chosen most often to be linear in n and x . Then the second term from (3.6) is replaced by

$$\varphi(x) \exp[-2\bar{v}t - i\sqrt{\bar{v}^2 + n^2 x^2 \alpha_0 t}].$$

In many cases the introduction of damping leads to deceleration of the instability development process, leaving it qualitatively the same in character.

4 FORMULATION OF THE LONGITUDINAL INSTABILITY MATHEMATICAL SIMULATION PROBLEM

In the domain of applicability of the model, the system of Eq. (2.17) is finite and consists of $2n_m + 1$ equations, where $n_m < R_0/r$, r is the minor radius of a ring. We shall assume that harmonics are not coherent and weakly excited when $n > n_m$ and, correspondingly, we shall put $\psi_{n > n_m} = 0$.

Let us set the following initial conditions for ψ_n (i.e., conditions when $t = 0$): we will choose the beam distribution function in the form of a Gaussian distribution with the semi-width $\langle W_0 \rangle$ (initial beam dispersion); it is normalized according to (2.29):

$$\psi_0(W)|_{t=0} = \frac{N}{(2\pi)^{3/2} \langle W_0 \rangle} \exp\left[\frac{-W^2}{2\langle W_0 \rangle^2}\right]. \quad (4.1)$$

We assume that at the initial stage the linear theory is valid, so that the initial value $\psi_{n \neq 0}$ can be expressed through ψ_0 using (3.3). We assume, also, that the initial level of the disturbing fields is sufficiently small.

For the numerical study it is important to choose a convenient set of dimensionless variables. Let us define

$$x = \frac{W}{\langle \tilde{W} \rangle}; \quad \tau = \tilde{\gamma} t; \quad \bar{\psi}_n = \frac{\langle \tilde{W} \rangle}{N} \psi_n; \quad (4.2)$$

$$\bar{\lambda}_n = \frac{\lambda_n}{N}; \quad \eta_n = \frac{Z_n}{nZ_0}; \quad \delta_n = \frac{|\eta_n| - \eta_n''}{2}$$

Then system (2.17) takes the form

$$\begin{aligned} \partial_\tau \bar{\psi}_n(x) + in\alpha_0 x \bar{\psi}_n \frac{\langle \tilde{W} \rangle}{\tilde{\gamma}} \\ + \frac{1}{\tilde{\gamma}} \frac{2e^2 N}{R_0 \langle \tilde{W} \rangle} \sum_m m \eta_m \bar{\lambda}_m \partial_x \bar{\psi}_{n-m} = 0. \end{aligned} \quad (4.3)$$

We have omitted here the constant ω_0 , i.e., we assumed the distribution centered in ω_0 . Henceforth we shall omit dashes above the dimensionless variables.

Quantities $\langle \tilde{W} \rangle$ and $\tilde{\gamma}$ can be chosen in a number of ways. It is convenient to make the following choice:

$$\tilde{\gamma} = \tilde{n} \omega_0 \sqrt{\frac{2v}{\gamma_0}} \sqrt{\delta_{\tilde{n}}} \quad (4.4)$$

$$\langle \tilde{W} \rangle = \langle W_{cr\tilde{n}} \rangle = \frac{E_0}{\omega_0} \sqrt{\frac{2v}{\gamma_0}} \sqrt{\delta_{\tilde{n}}},$$

i.e., the time is normalized to the linear increment of the \tilde{n} th harmonic (for example, with maximal value of

$$\left| \frac{Z_n}{nZ_0} \right|;$$

then, in the case of free space, $\tilde{n} = 1$, and the instability threshold of the first harmonic is the only one to consider). The generalized moment is normalized to the critical dispersion for the \tilde{n} th harmonic, which is given here by (2.28). The convenience of this normalization is in the invariance of the system (4.3) with respect to the parameter $\sqrt{v/\gamma_0}$. Let the initial dispersion be m times smaller than the critical one:

$$\langle x_0 \rangle = \frac{\langle x_{cr} \rangle}{m}. \quad (4.5)$$

We can set the parameter m as *initial* counting parameter and get the evolution picture for any value of the parameters entering the quantity $\sqrt{v/\gamma_0}$: N , R_0 (or B —the retaining magnetic field), γ_0 —if $v/\gamma_0 \ll 1$ is valid. For example, one can

change N , the number of electrons in the ring; naturally, it will change [when (4.5) is fixed] the real values of the initial and critical dispersions, increments, and maximal evolution time $t_{\max} = \tau_{\max}/\tilde{\gamma}\tilde{n}$. Another advantage of the normalization (4.4) is that it is easy to find an *exact* instability threshold by studying the system numerically in the linear approximation, when some of the harmonics increase and some of them damp. The last statement is true if impedance is a regular function of n (for example, for the case of free space). In this case the quantity $\langle x_{cr} \rangle$ is given by the formula

$$\langle x_{cr} \rangle = \langle x_0 \rangle (n_i)^{1/3}, \quad (4.6)$$

where n_i is the number of increasing harmonics (for free space). Numerical experiments have proven the validity of the formulas (2.27) to (2.28). For example, for $m = \langle x_{cr} \rangle / \langle x_0 \rangle = 2$, n_i is exactly equal to 8. The main reason we worked mostly with Eq. (2.17) is that the exact Eq. (2.16) does not allow the “invariant” normalization. Finally, Eq. (4.3), which is the starting equation for the numerical calculations, takes the form

$$\partial_\tau \psi_n(x) = i \frac{n}{\tilde{n}} x \psi_n - 2\pi \sum_m \frac{m}{\tilde{n}} \frac{\eta_m}{\delta_{\tilde{n}}} \lambda_m \partial_x \psi_{n-m}, \quad (4.7)$$

where dimensionless variables [(4.2) (4.4)] were used.

Still another possibility would be to normalize to the total initial ring energy E_0 : $\langle \tilde{W} \rangle = E_0/\omega_0 = mcR_0\gamma_0$, and arbitrarily in time, for example $t = \tau/\omega_0$.

In most of the cases we used “invariant” normalization, because we were mainly interested in the study of the nonlinear interactions’ influence on the ring’s evolution and on the perturbing fields for different Z_n th and in different regimes (from strongly above-critical or hydrodynamical: $\langle W_0 \rangle \ll \langle W_{cr} \rangle$ to “near-threshold” ones: $\langle W_0 \rangle \lesssim \langle W_{cr} \rangle$; corresponding, or to $m = 10 \rightarrow m = 1.5$ [Eq. (4.5)]. We were also interested in the study of the possibility of the appearance of nonlinear stabilization.

In the dimensionless variables (4.2), (4.4), conservation of the number of particles takes the form

$$I_1 = 2\pi \int \psi_0(x, \tau) dx = 1 \quad (4.8)$$

and “differential conservation laws” [(2.25) to (2.26)] take the forms

$$\frac{d}{d\tau} \int x \psi_0 dx = 2\pi \sum_m \frac{m}{\tilde{m}} \frac{\eta'_m}{\delta_{\tilde{m}}} |\lambda_m|^2 \quad (4.9)$$

$$\begin{aligned} \frac{d}{d\tau} \left[\int x^2 \psi_0 dx - 2\pi \sum_n \frac{\eta_n''}{\delta_{\tilde{n}}} |\lambda_n|^2 \right] \\ = 4\pi \sum_n \frac{n \eta_n'}{\tilde{n} \delta_{\tilde{n}}} \lambda_n \int x \psi_{-n} dx. \end{aligned} \quad (4.10)$$

Expressions [(4.8) to (4.10)] are invariant with respect to the ring's parameters N , R_0 , γ_0 , and their validity was checked at every step in time during the numerical calculations. In the same variables and in the same approximation $|\alpha_0 W/\omega_0| \ll 1$ the expressions for the energy and radiation power are

$$\begin{aligned} E(\tau) = 2\pi N E_0 \left[\int \psi_0 dx + \sqrt{\frac{2v}{\gamma_0}} \delta_{\tilde{n}} \int x \psi_0 dx \right. \\ \left. - \frac{v}{\gamma_0} \delta_{\tilde{n}} \int x^2 \psi_0 dx - 2\pi \frac{v}{\gamma_0} \sum \eta_n'' |\lambda_n|^2 \right], \end{aligned} \quad (4.11)$$

$$\begin{aligned} \frac{d}{d\tau} E = 4\pi^2 N E_0 \left[\sqrt{\frac{2v}{\gamma_0}} \sum \frac{n \eta_n'}{\tilde{n} \sqrt{\delta_{\tilde{n}}}} |\lambda_n|^2 \right. \\ \left. - \frac{2v}{\gamma_0} \sum \frac{n \eta_n'}{\tilde{n}} \lambda_n \int x \psi_{-n} dx \right], \end{aligned} \quad (4.12)$$

and the exact relation (2.25) is

$$\begin{aligned} \frac{d}{d\tau} \left\{ 2\pi N E_0 \left[\int \psi_0 \sqrt{1 + \sqrt{\frac{v}{\gamma_0}} \sqrt{\delta_{\tilde{n}}} x} dx \right. \right. \\ \left. \left. - 2\pi \frac{v}{\gamma_0} \sum \eta_n'' |\lambda_n|^2 \right] \right\} = 8\pi^2 N E_0 \sum \frac{n \eta_n'}{\tilde{n} \sqrt{\delta_{\tilde{n}}}} \lambda_n \\ \times \int \left(1 + 2 \sqrt{\frac{v}{\gamma_0}} \sqrt{\delta_{\tilde{n}}} x \right)^{-1/2} \psi_{-n} dx. \end{aligned} \quad (4.13)$$

The last three expressions are not invariant with respect to the ring's parameters.

In the numerical experiments, relations [(4.8) to (4.13)] were fulfilled with an accuracy better than 10^{-5} during the calculations, before the distribution left the domain of numerical consideration due to divergence of the solution.

The differential approximating method (4.7) was chosen to be the same as in Ref. 14 (where the approximation was justified and stability proven). We used 10 harmonics for the calculations, assuming that, according to the initial assumptions, for $n > 10$ fields are incoherent. The limitation of n to 10 is related to the computer capacity (in particular, calculations for one variant take from 4 to 7 hours of the CDC-6200 computer time, depending on the parameters chosen).

5 RING IN FREE SPACE

We consider the longitudinal instability of RER for the easiest case of free space. In this case the impedance is a regular function of n :

$$\left| \frac{Z_n}{n Z_0} \right| = n^{-2/3}.$$

More specifically¹²

$$Z_n = \pi n^{1/3} Z_0 \cdot 0.26 \left(-1 - \frac{\sqrt{3}}{3} i \right). \quad (5.1)$$

Formula (5.1) is valid with good accuracy for $n \geq 5$; for $n = 1, \dots, 4$ more accurate values of Z_n are obtained by numerical calculation.¹⁴ Note that in Ref. 14 the wrong sign of Z_n'' was used, which leads, according to (2.27), to a rather strong decrease of the increment. When the initial dispersion is

$$\langle x_0 \rangle < \langle x_{cr} \rangle \cdot 10^{-1/3} \approx 0.47 \langle x_{cr} \rangle \quad (5.2)$$

we find from (4.6) that all 10 harmonics, which we consider, are unstable. This was also confirmed in the numerical experiment.

We shall describe two most significant experiments: the strongly above-critical regime ($\langle x_0 \rangle = 0.2 \langle x_{cr} \rangle$) and the "near-threshold" one ($\langle x_0 \rangle = 0.58 \langle x_{cr} \rangle$).

a) $\langle x_0 \rangle = 0.2 \langle x_{cr} \rangle$. The growth of the quantities $|\lambda_n| \sim |\mathcal{E}_n|/|Z_n|$ (2.15) was in excellent agreement with Eq. (2.27) at the initial linear stage of the instability development. For $n = 3, 4$, when τ was increased by 1, the amplitude ratio $|\lambda_n|$ gave the number $n^{2/3}e$ with three figure accuracy. For $n = 1$ the increment was slightly bigger than the value given by the theory, and for $n = 8$ to 10 it was slightly smaller. The difference was increasing in time. This phenomenon will be explained later. Figure 1a presents graphs of $|\lambda_n(t)|$ for $n = 1, 3, 5, 7, 10$. Linear exponential growth transforms in time into oscillations with an average amplitude, which is more than an order of magnitude smaller than that obtained from the estimating formula (2.29). The speed of the evolution process is maximal for the 10th harmonic, which has the maximal increment. We note also that the maximum of the amplitude for $n = 1$ is higher than the corresponding maxima for $n = 2$ to 9, and comparable with the maximum for $n = 10$.

Figures 1b and 1d show the behaviour in time of the field's energy in the ring $E_i(\tau)$ [term E_i in (2.20)], radiation power $dE/d\tau$ (4.12), energy dispersion in the ring $\langle W \rangle$, and derivative $d\langle W \rangle/d\tau$

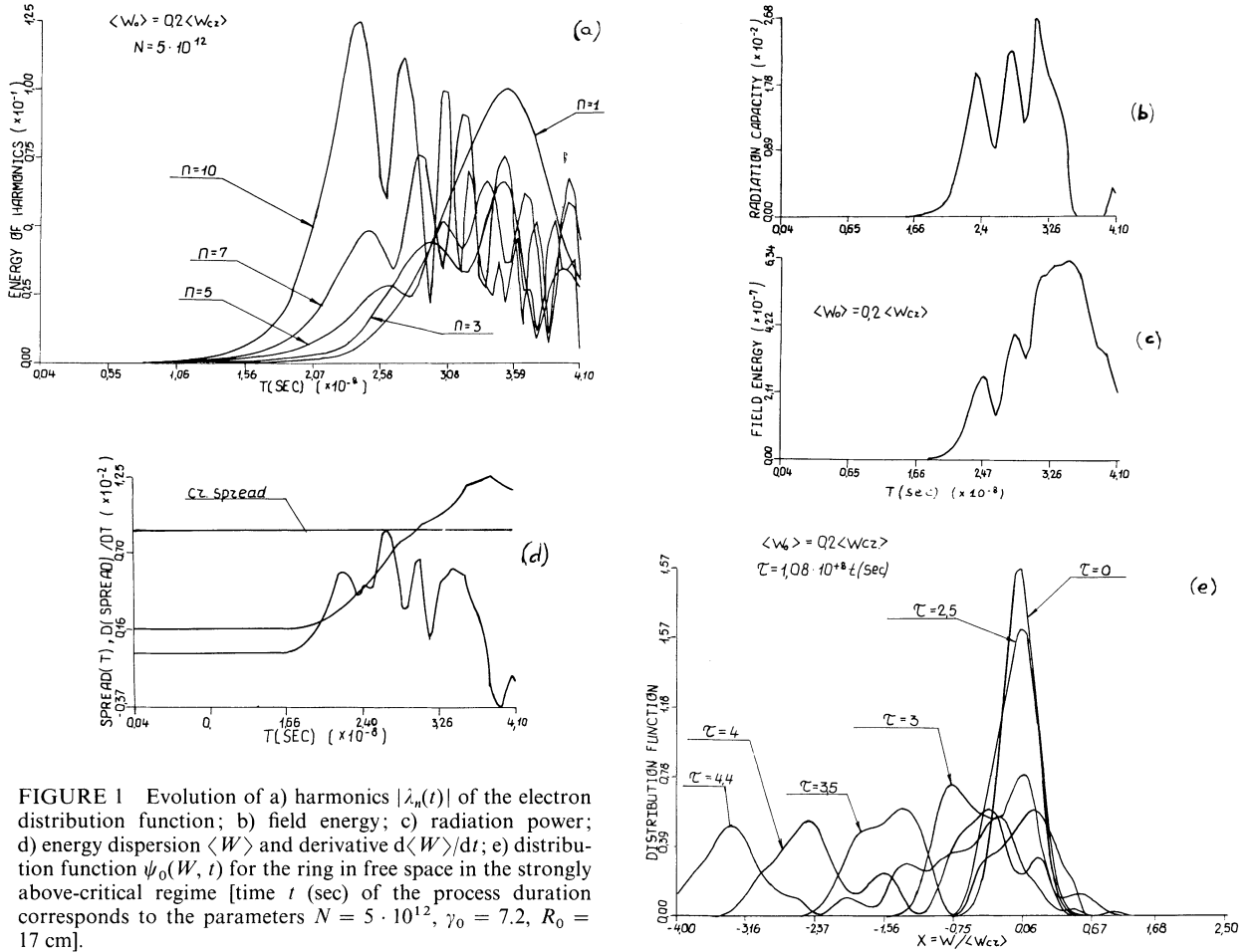


FIGURE 1 Evolution of a) harmonics $|\lambda_n(t)|$ of the electron distribution function; b) field energy; c) radiation power; d) energy dispersion $\langle W \rangle$ and derivative $d\langle W \rangle/dt$; e) distribution function $\psi_0(W, t)$ for the ring in free space in the strongly above-critical regime [time t (sec) of the process duration corresponds to the parameters $N = 5 \cdot 10^{12}$, $\gamma_0 = 7.2$, $R_0 = 17$ cm].

for $\sqrt{v/\gamma_0} = 0.043$ ($\gamma_0 = 7.2$; $R_0 = 17$ cm; $N = 5 \cdot 10^{12}$).

During the initial period, the behaviour of $E_i(\tau)$ is analogous to the behaviour of $|\lambda_n(\tau)|$ for large n ; when $\tau = 3$ a new "bend" appears, then $E_i(\tau)$ oscillates with increasing amplitude. In the experiment described, calculations were stopped at $\tau = 4.4$, because the ring was broadened so much that the graph of $\psi_0(x)$ fell outside the limits of the numerical domain considered. An interesting fact is that the curve for the radiation power $dE/d\tau$ is very close in its form to the energy curve $E_i(\tau)$ (exceeding it by more than 4 orders of magnitude). Also $d\langle x \rangle/d\tau$ has similar time behaviour. By the end of the calculation, the amount of energy radiated by the ring (at the above-given values of parameters) was 20% of the total ring's energy. Correspondingly, the field energy in the ring is $E_i|_{\tau=4.4} = 0.003\%$, evolution time $t = 4 \cdot 10^{-8}$ sec.

Figure 1e represents graphs of $\psi_0(x)$ at the moments $\tau = 0, 2.5, 3, 3.5, 4, 4.4$. The behaviour of $\psi_0(x, \tau)$ agrees very satisfactorily with the qualitative consideration from Section 3. By the time $\tau = 4.4$ the ring fell apart completely, and calculation was stopped. The final value of the dispersion was $\langle x \rangle = 0.15$ $\langle x_0 \rangle = 1.23 \langle x_{cr} \rangle$.

The conclusion, which follows from the above, is that in the given model, when the initial dispersion is much smaller than the critical one, the ring falls apart in free space in a very short time, $t < 10^{-7}$ sec.

What can be done to overcome this situation and to get a relatively stable ring for a relatively long time? A rather radical possibility will be considered in the next section. For the present, let us analyze the approximations used in our model. From the above results it is clear that nonlinear interactions become very effective, and even determining, when harmonic amplitudes

reach a certain level. Then they limit the level of the perturbing fields. (Note that in the linear approximation harmonics rise without limit.) We completely neglect harmonics with $n > 10$, assuming that they are incoherent. Incoherency leads to a strong decrease of the instability increment. One may consider the case when incoherent harmonics are in a stable regime: then nonlinear interactions could effectively pump the energy from the unstable modes, which would lead to the nonlinear stabilization of the instability. More precisely, by nonlinear stabilization we understand *strong reduction of speed of instability development* due to the nonlinear interactions. It is clear that one cannot get an absolutely stable ring, one which would not "crawl away" in the above-critical regime, because, as the final result, turbulent energy gets dissipated, leading to the heating of the ring and increasing its dispersion. This is true if at least one harmonic is unstable. However, nonlinear

interactions could *very considerably* slow down this process, when parameters are optimally chosen. For this it would be necessary to have *primary direction of pumping towards high harmonics*.

b) Let us consider now the "near-threshold" regime $\langle x_0 \rangle = 0.58 \langle x_{cr} \rangle$. In this case for $n > 5$ the harmonics damp, and for $n \leq 5$ the increment decreases. Figure 2 is analogous to Figure 1 in the previous case, if the values of the parameters are the same. The speed of the process as a whole is considerably smaller (about 4 times). Before $\tau = 12-13$, lower harmonics grow approximately according to the linear theory, then they start to cut off, and from this moment higher harmonics, which were fluctuating irregularly near the average value $\sim 10^{-5}$, start impetuous, "explosive" growths.

Approximately from the same moment starts a fast broadening and "shifting" of the distribution function $\psi_0(x)$, accompanied by a sharp increase in the radiation. After $\tau = 20$ the calculation was

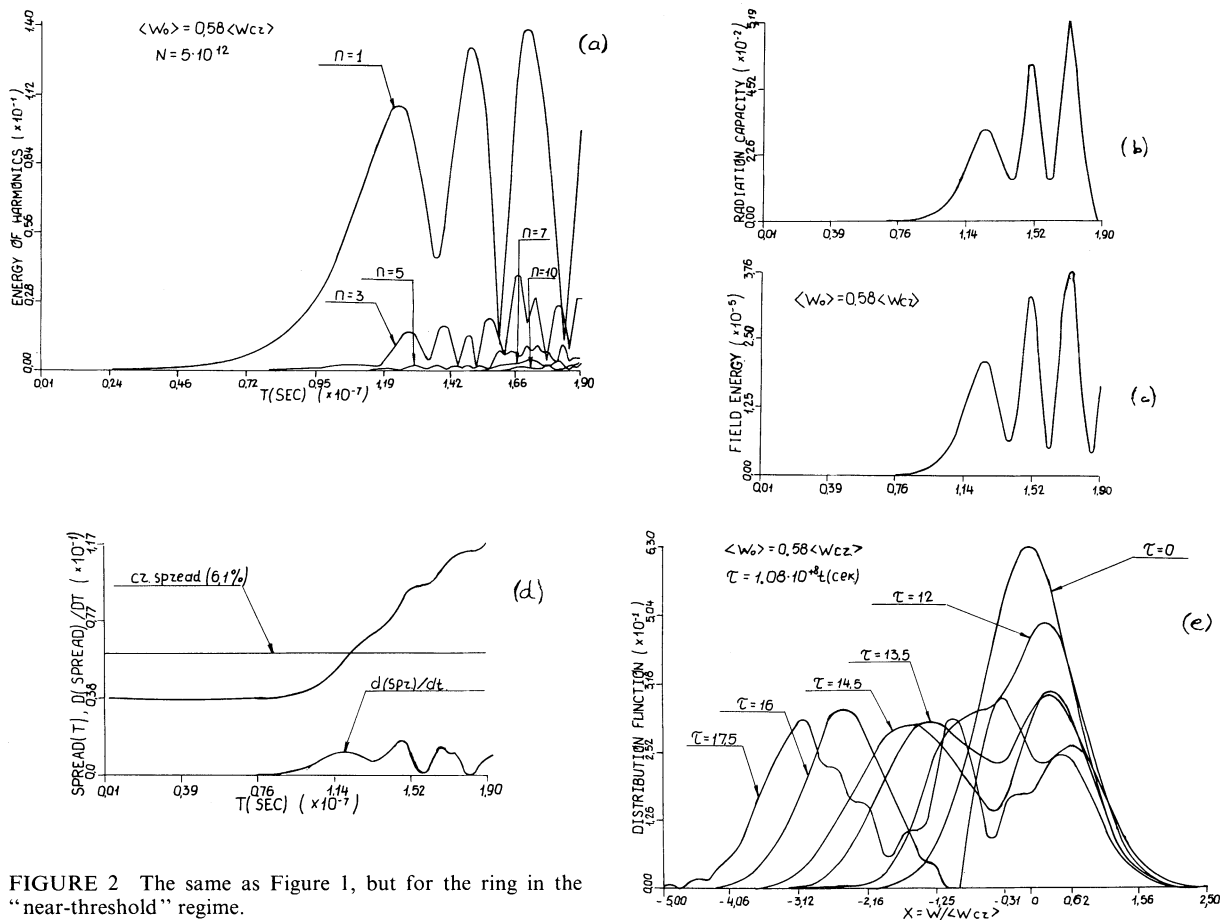


FIGURE 2 The same as Figure 1, but for the ring in the "near-threshold" regime.

stopped, because the ring fell apart, its effective dispersion exceeded the critical one, and clearly the further course of the process must be completely analogous to the one considered in the previous case.

High efficiency of the nonlinear interactions was shown in the example considered with respect to the pumping of the energy from some modes to others. Clearly, if we would take into account incoherent harmonics, this would lead to even stronger retardation of the process. However, the instability development time, obtained here ($t = 1.9 \cdot 10^{-7}$ sec) is too small to satisfy the requirements of the experimentalists. The time gets still smaller when the number of particles in the ring N increases.

From the results presented above it follows that there exists pumping of the energy towards high harmonics if the amplitude difference is large enough. However, in both cases considered, the speed of growth of the first harmonic is accelerated. The following numerical experiment was set up in order to determine accurately the preferential direction of pumping: the evolution of the solutions of the system (4.7) in the purely nonlinear regime (with linear terms thrown out) was considered for $n = 1, 2, 9, 10$ and initial conditions $|\lambda_n| = 10^{-2}$ for $n = 1, 2$, $|\lambda_n| = 10^{-4}$ for $n = 9, 10$, and vice versa. In both cases increase of $|\lambda_1|$, $|\lambda_2|$ and damping of $|\lambda_9|$, $|\lambda_{10}|$ took place. From this it follows that there exists *the preferential direction of nonlinear pumping towards smaller n 's*, mostly into the first harmonic, which explains the above-mentioned increase in growth of the lower harmonics. Consequently, it is *advantageous to create a negative gradient in the direction of smaller n 's*. Such a case will be considered in the next section.

The main conclusion from the results of this section is the following: in the frame of the given model, in free space, even with initial dispersion not much smaller than the critical one, the ring spreads apart and reaches a dispersion which is equal or larger than the critical one in a time less than $t < 5 \cdot 10^{-7}$ sec, and the efficiency of nonlinear stabilization is insufficient to hold the instability to a reasonable level.

6 THE RING IN THE RESONATOR

In the real experimental settings the relativistic beam is injected into a chamber referred to as a resonator, or adhesator, or compressor, in which it forms a ring; then the ring is compressed by the

external fields to the required radius R before its introduction into the accelerating system. When the initial dispersion is small enough, the instability may start to develop even during the injection. Therefore, the first step in studying the ring's behaviour under real experimental conditions is to consider the ring's instability in the resonator. The only experiments with which we are acquainted, in which concrete parameters of the ring's instability in the resonator were measured, are described in Refs. 10 and 11. Measured parameters were: radiation power, time of the instability development, final energy dispersion as a function of the number of particles in the ring, initial dispersion, and harmonic numbers.

We will now consider the specific values of the parameters of the experiment:¹¹ $\gamma_0 = 7.2$, $R_0 = 17$ cm (injection radius), figures of merit of the chamber $Q = 10$, $N = 10^{11} - 7 \cdot 10^{12}$. The parameter $\sqrt{v/\gamma_0}$ was changing correspondingly between the limits $6.3 \cdot 10^{-3}$ to $5 \cdot 10^{-2}$, i.e., the results of the experiment can be compared with the calculations in the frame of the given model. The impedance dependence of the harmonic number n is different from the case of free space and is much more complicated, which is of principal importance here. Figure 3 shows a qualitative graph of the $|Z_n/n|$ dependence on n along with the graphs of $|Z_n/n|$ for the ring in a free space and in the space between two infinite conducting walls, taken from Ref. 11. (In the experiment described in Ref. 11, the chamber had the shape of a cylinder with a height $h = 5$ cm and radius $R = 22$ cm.) It is seen that the main effect of the chamber is to damp the impedance modulus strongly when n 's are small ($n < 10$), compared to the free space, and to raise $|Z_n/n|$ for $n > 10$ when the frequencies of the ring's perturbing fields start to coincide with the frequencies of the normal modes of the chamber, i.e., when the resonance conditions are satisfied. For us not only the n -dependence of the impedance modulus is important, but also the n -dependence of the real and imaginary parts of Z_n , which is not given in Ref. 11. The beam impedance in chambers was studied in Ref. 5 (for the case of an infinitely long conducting tube) and in Ref. 17 (for the ring in a resonator). Expressions for Z_n were obtained in the form of infinite series. The characteristic feature of these expressions is that the modulus of the real part of the impedance increases strongly at resonance (roughly speaking, proportionally to the chamber's figure of merit), and that Z_n' changes its sign in the resonance. If the figure of

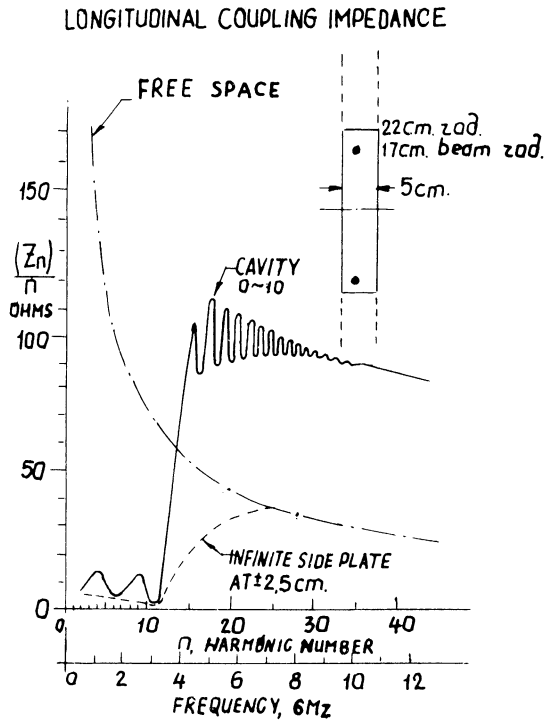


FIGURE 3 Approximate behaviour of the impedance of the ring's coupling $|Z_n/n|$ in a) free space; b) between infinite conducting walls; c) in the chamber (resonator).

merit is high, resonances are very narrow and relatively well separated; when Q is small, they overlap and for $|Z_n/n|$ we have a picture similar to that given in Figure 3.

In Figure 4, graphs of the functions Z'/nZ_0 , Z''/nZ_0 , $|Z_n/nZ_0|$ are presented. They were calculated using the program for the impedance calculations† with $R_0 = 17$ cm, $h = 5$ cm, $R_b = 22$ cm and with figure of merit values taken to be $Q = 10, 20$. It is seen that for $n > 10$ the result differs considerably from the corresponding graph in Figure 3—the number of resonances is small, and they are strongly separated. The difference could be due to the fact that the chamber in the experiment¹¹ had more complicated geometry—special “holes” were made in it in order to artificially lower the figure of merit. Nevertheless, important information can be extracted from Figure 4—namely, the behavior of Z'_n and Z''_n in the neighbourhood

† The authors are grateful to N. Yu. Kazarinov for permission to use his program for the impedance in the resonator calculations. In the above-mentioned program a procedure of partial series summation is used for the series from the analytical expression of the impedance, neglecting the conductivity of the cylindrical wall.

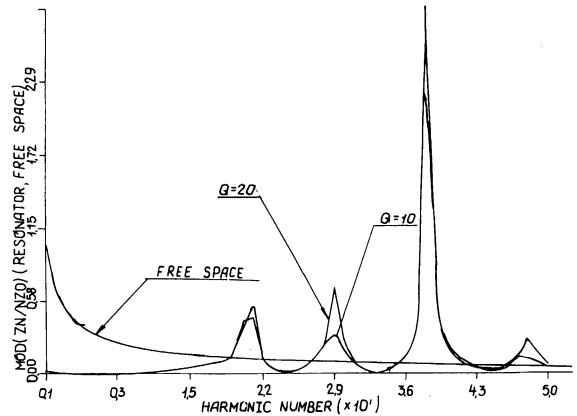


FIGURE 4 Modulus Z_n/nZ_0 for the ring in the chamber ($h = 5$ cm, $R_b = 22$ cm, $R_0 = 17$ cm, $Q = 10, 20$), calculated on the computer.

of the resonances; in particular the characteristic change of the sign of Z''_n .

The important results of the experiments, which the authors of Ref. 11 could not explain theoretically, were:

a) The small deviation of the final energy dispersion ΔE from the initial energy dispersion ΔE_0 , when the number of particles in the beam was varied within the wide limits (10^{11} to $7 \cdot 10^{12}$) [when $(\Delta E/E)_0 = 1\%, 2\%$].

b) The complete stopping of radiation of energy by the ring after the splash of radiation when the dispersion was still smaller than the critical one. For large N the quantities ΔE_0^{-1} were considerably larger than ΔE_{cr}^{-1} .

In the frame of our model and our understanding of the process of the instability development, supported by the results of the previous section, we may try to explain the above results by strong damping of the instability due to the nonlinear pumping of energy of the excited harmonics ($n > 15$) into lower harmonics, which are below the instability threshold when $(\Delta E/E)_0 = 1\%, 2\%$, and keeping in mind the preferential direction of pumping towards smaller n . [In the case of $(\Delta E/E)_0 = 0.1\%$ the beam in the experiment¹¹ evolved to the dispersion $\sim 6\%$ when $N = 7 \cdot 10^{12}$, in agreement with theoretical predictions.] We consider the model in which, again, 10 harmonics are taken into account, and Z_n/nZ_0 is shown on Figure 5. This model impedance was constructed by combining the results of the described numerical calculations of Z_n and the general notion of the $|Z_n/n|$ behaviour in the experiment. The regime

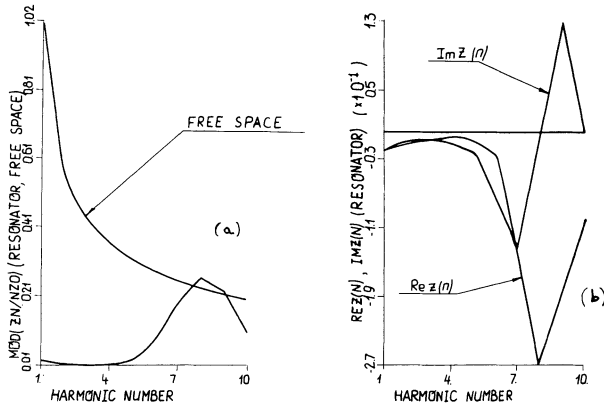


FIGURE 5 a) Module; b) real and imaginary parts of the "model" impedance Z_n in the chamber.

with initial dispersion for the 8th harmonic exceeding the critical one by a factor of two was considered. Formulas (2.27) to (2.28) for increments and thresholds were used. Then the 9th harmonic, for example, must grow with a considerably smaller increment than that of the 7th (due to the $Z_9'' > 0$), although they have very close values of $|Z_n|$. This

was supported by the result of a numerical experiment. The first harmonics are damped in the linear approximation.

Let us note that this model can be realized in the experiment if one chooses parameters so that the first resonance corresponds to $n = 8$, and harmonics with $n > 10$ are incoherent.

The results of the corresponding numerical experiment are presented in Figure 6.

Figure 6a shows changes of $|\lambda_n|$ in time for $n = 1, 2, 7, 8, 9, 10$. The picture is similar to the one in the previous section, if we interchange lower and higher harmonics. The most unstable harmonics are stabilized when a certain energy level is reached. But due to the nonlinear processes, intensive energy pumping into stable harmonics takes place, which leads to their sharp growth. Note, again,

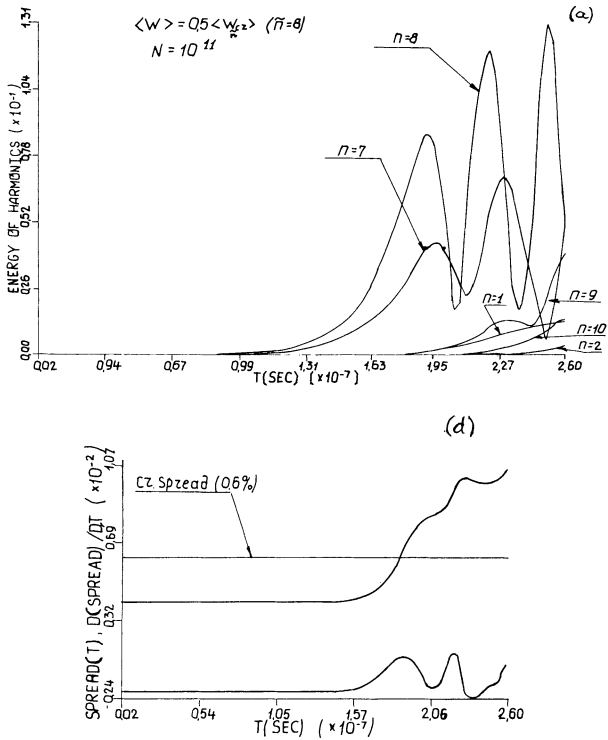
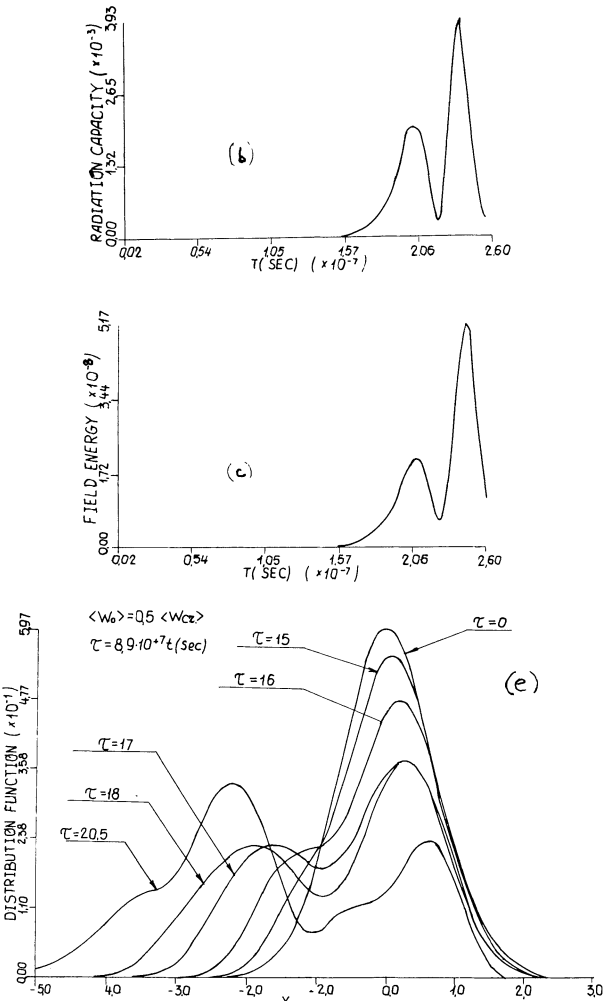


FIGURE 6 The same as Figure 1, for the ring in the chamber with model impedance ($\gamma_0 = 7.2, R_0 = 17$ cm, $\langle W_0 \rangle = 0.5 \langle W_{cr} \rangle, N = 10^{11}$).



that the most intensive pumping goes into the first harmonic; the beginning of the sharp growth of lower harmonics shifts in time with growth. When $\tau = 14$ ($\bar{n} = 8$), rapid growth of the field amplitude E_i and of the radiation power starts, as well as broadening of the ring. After a few oscillations, the field E_i [with amplitude maximum 20 times smaller than is given by (2.29)] is decreased by an order of magnitude when $\tau = 21$. The radiation power decreases correspondingly, i.e., the ring, which lost part of its energy, produces much less radiation. The final dispersion is more than two times larger than the initial, and 1.22 times larger than the critical one. It is interesting to compare the results obtained with the results of the experiment. The radiation power behaves in time very similarly — one has almost complete stopping of the radiation after the splash. The best fit is obtained when $N = 10^{11}$. Then the time of the process duration is $t = 2.4 \cdot 10^{-7}$ sec, which is close enough to the experimentally determined maximal time $t < 10^{-6}$ sec. The final dispersion of 1.1%, with initial dispersion of 0.5% does not correspond very well to the experimentally determined dispersion of 0.75%. Nevertheless, the agreement is satisfactory for the rough assumptions made (model form of the impedance and neglect of the incoherent harmonics' influence).

It is clear that if we now pass to "nonvariant" normalization (see Section 4), fix the dispersion (for example, at 1%) and increase the number of particles in the ring, then $\langle x_{cr} \rangle$ and the ratio $\langle x_{cr} \rangle / \langle x_0 \rangle$ will both increase correspondingly. The process will go as was described above: the dispersion will come at least to its critical value, which is in contradiction with the weak dependence of the final dispersion on the critical one when $(\Delta E/E)_0 > 0.5\%$, as was observed in the experiment.¹¹ We suggest the following qualitative explanation of this phenomenon. Let us recall that the imaginary part of the impedance is changing sign when passing through the resonance. According to the formulas (2.27) to (2.28), in the region $Z_n'' > 0$ the increment is strongly decreasing, and the instability threshold correspondingly.

The ring is losing energy by radiation, and its average radius is decreasing correspondingly. But the form of the curve $Z(n)$ and location of the resonances are very sensitive to the differences of the average ring radius. The graphs of $|Z_n/nZ_0|$, Z_n'/nZ_0 , and Z_n''/nZ_0 were calculated using the above-described program, and they are presented in Figure 7 for $R_0 = 17$ cm and $R = 16.6$ cm.

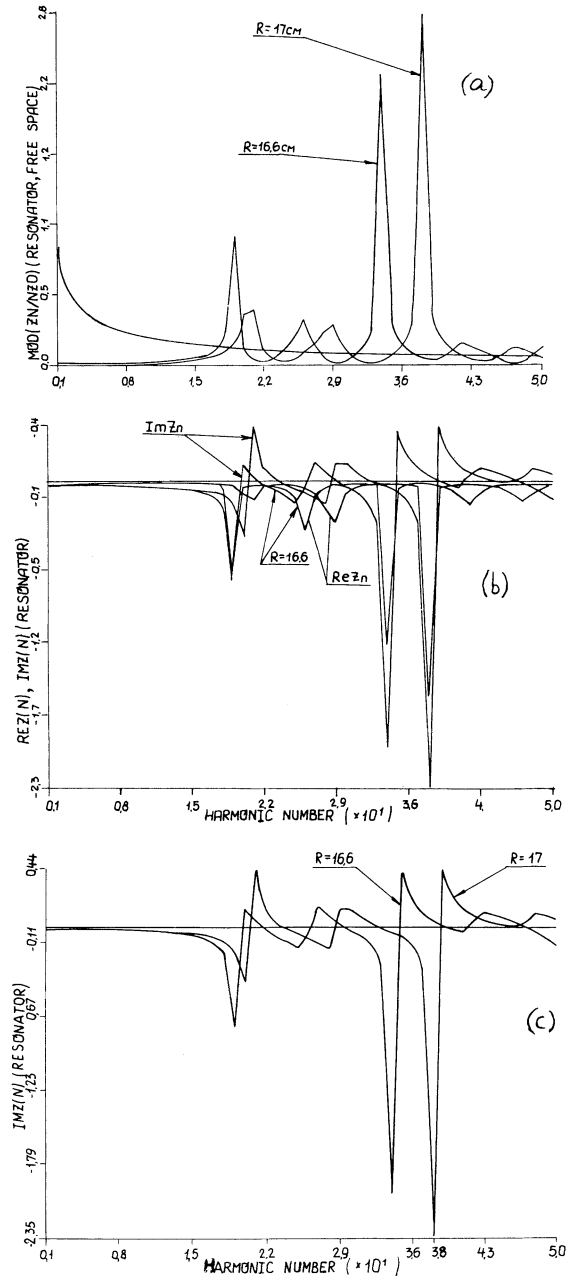


FIGURE 7 a) Module; b) real and imaginary parts; c) imaginary part Z_n/nZ_0 for the ring in the chamber with $R = 17$ cm, 16.6 cm.

Radius 16.6 cm corresponds to the ring's energy loss of only 2.5% (when $R_0 = 17$ cm). It can be seen from Fig. 7 that resonances were shifted towards small n 's, and on the 38th harmonic the increment decreased by a factor of 40, in accordance to (2.27).

Thus the 38th harmonic was moved to the stable region with a moderate excess of its dispersion over the critical one. On the other hand, the increments for $n > 38$ were correspondingly increased. The resonance at $n = 38$ was shifted more strongly than the one at $n = 21$. When resonances are moving thus, control of the instability of the excited harmonics takes place and effective instability stabilization may appear, which would lead to the significant increase of its development time. The effect described is reminiscent of the phenomenon of quasi-linear relaxation.

Therefore, there remains the self-consistent problem of unstable beam behaviour in the chamber and impedance, which awaits solution.

The main conclusions of our study are the following: the numerical study of the instability of the RER in the resonator in the thin ring model in many cases leads to results which are in reasonable agreement with experiment. Better agreement can be obtained if one takes into account more harmonics (in particular, incoherent ones), and the effect of resonance shifting.

ACKNOWLEDGMENTS

The authors are sincerely grateful to Yu. I. Aleksahin, N. Yu. Kazarinov, and E. A. Perelstein for numerous useful discussions, and E. P. Zhidkov and M. G. Meshcheryakov for support.

REFERENCES

1. V. I. Veksler, V. P. Sarantsev, *et al.*, Collective linear acceleration of ions, *Proc. 6th Intern. Conf. on High-Energy Accelerators*, Cambridge, Mass., USA, 1967, p. 289.
2. A. G. Bonch-Osmolovskii *et al.*, JINR Report P9-4138, Dubna, 1968.
3. A. A. Kolomenskii and A. N. Lebedev, *Atomnaya Energia* **7**, 549 (1959); C. Nielsen, A. Sessler, and K. Symon, in the collection of works *Storage of Relativistic Particles* (Atomizdat, Moscow, 1963).
4. R. Briggs, *Symp. on Electron Ring Accelerators*, Berkeley, 1968, p. 434. A. G. Gaponov, *Izv. VUZov* (University Bulletin), *Radiophysics* **11**, 836 (1959).
5. A. G. Bonch-Osmolovskii and E. P. Perelstein, *Izv. VUZov, Radiophysics* **13**, 1081, 1089 (1970).
6. D. Möhl, L. J. Laslett, and A. M. Sessler, Report on Dubna Symposium. Preprint LBL-1062, Berkeley, 1972.
7. V. G. Makhankov and M. G. Mesheryakov, *Atomnaya Energia* **36**, 78 (1974).
8. B. S. Getmanov, V. G. Makhankov, and M. G. Mesheryakov, *Proc. of IV All-Union Conf. on Charged Particle Accelerators*, Moscow, 1974.
9. B. W. Stallard and R. B. Weiss, *Bull. Am. Phys. Soc. Ser. 2*, **13**, 114 (1968).
10. U. Schumacher *et al.*, *Proc. of IV All-Union Conf. on Charged Particle Accelerators*, Moscow, 1974.
11. A. Faltens *et al.*, *Proc. Ninth Intern. Conf. on High Energy Accelerators*, Stanford, 1974, p. 226.
12. A. G. Bonch-Osmolovskii and V. N. Tsytovich, *Trans. of the FIAN* (Lebedev Inst. of Phys., Acad. of Sci.) **66**, 144 (1973).
13. C. Pellegrini and A. M. Sessler, Preprint LBL, ERAN-203, Berkeley, 1973.
14. B. G. Shchinov *et al.*, *Plasma Phys.* **15**, 211 (1973).
15. B. S. Getmanov, JINR Report P9-9244, Dubna, 1975.
16. S. Ishimaru, *The Basic Principles of Plasma Physics* (Atomizdat, Moscow, 1975).
17. Yu. I. Aleksachin, I. L. Korenev, and P. A. Yudin, JINR Report P9-7065, Dubna, 1973.